NASA

Technical Memorandum 82156

Fourier Spectroscopy on Planetary Missions Including Voyager

Rudolf A. Hanel

JUNE 1981

National Aeronautics and Space Administration

Goddard Space Flight Center
Greenbelt, Maryland 20771

Fourier spectroscopy on planetary missions including Voyager

Rudolf A. Hanel

Laboratory for Extraterrestrial Physics, NASA/Goddard Space Flight Center
Greenbelt, Maryland 20771

Abstract

In the last dozen years spaceborne Fourier Transform Spectrometers have obtained infrared emission spectra of Earth, Mars, Jupiter, Saturn and Titan as well as of the Galilean and other Saturnian satellites and Saturn's rings. Intercomparisons of the properties of planetary atmospheres and of the characteristics of solid surfaces are now feasible. The principles of remotely sensing the environment on a planetary body are discussed. Special consideration is given to the most recent results obtained by the Voyager infrared investigation on the Saturn system.

Introduction

For more than a decade spaceborne Fourier transform spectrometers have explored the Earth and other objects in the solar system. Michelson interferometers flown on Nimbus 3 in 1969[1,2] and on Nimbus 4 in 1970[3,4,5] recorded more than a million spectra of the Earth's atmosphere. More recently, a Russian meteorological satellite observed Earth with a similar type of interferometer constructed in East Germany.[6] An advanced version of the Nimbus instrument was flown on the Mariner 9 orbiter in 1971/72, allowing investigation of the infrared spectrum of Mars.[7,8,9] In 1979 the two Voyager spacecraft transmitted numerous spectra of Jupiter, Amalthea, and the Galilean satellites.[10,11,12] In November 1980, Voyager 1 passed through the Saturnian system and observed the planet, its rings, Titan and several other satellites.[13] Under present plans, Voyager 2 will fly by Saturn in August 1981, pass Uranus in 1986, and arrive at Neptune in 1989.

These space ventures have demonstrated the power of remote sensing with Fourier transform spectrometers. The wide spectral range at moderately high spectral resolution, the precise wavenumber and radiometric calibrations, and the reliability achieved by these instruments, have permitted scientific investigations which would otherwise have been impossible.

Weight limitations and the long flight durations prohibited the use of highly sensitive, cryogenically cooled detectors on these missions. Thermistor bolometers and thermopiles were used at ambient instrument temperatures. Even the best of these thermal detectors is far from being background-noise limited; therefore, the multiplex advantage of the Michelson interferometer was fully realized. The second important property of Michelson interferometers, the large throughput or area-times-solid-angle, was also used advantageously. The half-meter telescope of the Voyager IRIS was designed to match the $A\Omega$ of the interferometer and feed it with minimum losses. The third advantage of the Michelson interferometer over conventional techniques is its wavenumber precision. The spectra, shown in Fig. 1, of five solar system bodies with substantial atmospheres were recorded years apart by different instruments on different spacecraft, but the corresponding spectral features of CO_2 and H_2O on Earth and Mars, for example, and of CH_4 on Earth, the giant planets and Titan, fall precisely at the correct wavenumbers. This precision is of great help in identifying unknown constituents. Finally, the results from all missions have shown that interferometers can be calibrated in an absolute sense at least as well as conventional radiometers. The usual method of calibration of an infrared instrument in space is to expose the field of view to blackbodies of different temperature. In the case of the interferometer, each narrow spectral interval is calibrated independently. In contrast, the calibration of a radiometer applies to the entire passband of the instrument. A wavenumber dependent change of responsivity within this band could pass unrecognized in a radiometer but would be detected in the interferometer calibration. A method was developed on Voyager which allowed calibration of the whole system including the telescope, simply by viewing deep space occasionally and thermostating the entire instrument; no moving parts were involved.

In this talk I will give a brief review of the evolution of the instruments known as IRIS (InfraRed Interferometric Spectrometer). I will then discuss the concept of remote sensing by infrared emission spectroscopy, and show examples of results obtained with IRIS. Finally, I will discuss the most recent results from Voyager with emphasis on those from Titan, showing that the ability to record a wide spectral range with good spectral and spatial resolution and high radiometric accuracy has contributed substantially to our new understanding of this most interesting companion of Saturn.

The infrared interferometric spectrometer (IRIS)

The first Nimbus interferometer was patterned after a breadboard which was constructed by L. Chaney from the University of Michigan and our group at the Goddard Space Flight Center. After a successful balloon flight[14] and extensive laboratory testing,[15] the Michigan team pursued further balloon activities and the GSFC team space application. The conceptual layout of the interferometer is indicated in Fig. 2. Texas Instruments, Inc. in Dallas, Texas, built all of the space flight versions of the instrument.

The first launch in 1968 was a disaster due to a malfunction in the guidance system of the rocket. Months later, the U.S. Navy found badly corroded remnants of the spacecraft in the Pacific Ocean. A year later, Nimbus 3 was launched with a spare model of IRIS[16] on board and achieved the desired polar orbit. The interferometer functioned well and the mission was a success. A conventional grating spectrometer, SIRS,[17] and IRIS[2,18] obtained vertical temperature profiles of the atmosphere; in addition, IRIS obtained water vapor and ozone distributions. Today similar measurements are carried out routinely by operational weather satellites.

On Nimbus 4 the resolved spectral interval was decreased from 5 to 2.8 cm^{-1} and several other design changes contributed to the generally better performance of this instrument, as compared to its predecessor.[19] After a year's operation, the instrument was turned off because we were inundated by data.

A major design change was implemented in the next generation of IRIS, earmarked to fly on Mariner 8 and 9 to Mars.[20] In the Nimbus instrument, the potassium bromide beamsplitter material limited the spectral range to 400 cm^{-1}. However, the range between 200 and 400 cm^{-1} contains strong rotational water vapor lines, crucial to the Mars investigation. A change to cesium iodide was therefore made, although CsI is very soft, hard to polish and difficult to maintain flat. Again one of the two spacecraft, Mariner 8, was lost, this time in the Atlantic Ocean, but after a 6 month cruise Mariner 9 reached Mars and achieved the desired orbit. IRIS and the spacecraft performed beyond expectation, for eleven months, until the supply of attitude control gas was depleted.[7,8,9]

The largest and most ambitious step in the evolution of IRIS came in response to demanding requirements for exploration of the outer planets. Temperatures there are only slightly higher than that of liquid nitrogen; under these circumstances the measurement of the thermal emission spectrum is not an easy task. Moreover, the instruments had to survive for years in space and had to function in the severe high-energy particle environment which exists in the vicinity of Jupiter.

The optical layout of the Voyager IRIS is shown in Fig. 3.[21] The whole instrument, including the half-meter telescope, weighs only 18.4 kg and operates with an average power of 14 Watt. The Cassegrain telescope forms an image of the object at the focal plane aperture which limits the field of view to 0.25° full cone angle. A dichroic mirror channels the visible and near infrared portion of the spectrum into a radiometer, and the lower wavenumbers into the Michelson interferometer which analyzes the spectrum between 180 and 2500 cm^{-1} with a 4.3 cm^{-1} apodized resolution. The main interferometer and the reference interferometer, which controls the motor speed and the wavenumber calibration, are shown for convenience in Fig. 3 in the plane of the paper, although they are in reality perpendicular to it. As all previous IRIS, the Voyager instrument is thermostated by thermally insulating the entire assembly from the spacecraft, and allowing the instrument to cool by radiating to space. The instrument is held at a constant temperature of 200 K by the thermostatic action of small electrical heaters. Voyager IRIS has

three independent thermostats, one for the interferometer proper, one for the primary, and one for the secondary telescope mirror. The Voyager interferometers have performed well[21] although a slight optical misalignment, more pronounced on Voyager 2 than on 1, has been noted.

Remote sensing concept and results

The art of remote sensing is to infer physical and chemical conditions from radiance measurements at different wavenumbers and zenith angles. This task must be based on radiative transfer theory. The physical quantity measured by these interferometers is the spectral radiance expressed, for example, in W cm^{-2} sr^{-1} $(cm^{-1})^{-1}$. Sometimes it is more instructive, as in the case of Fig. 1, to plot the spectra in units of brightness temperature, defined as the temperature of a blackbody which emits, at a particular wavenumber, an equal amount of radiation as the object under investigation.

Restricting the case to thermal emission from a plane parallel atmosphere in thermodynamic equilibrium, of optical thickness τ_1, above a lower boundary of emissivity ϵ_G and temperature T_G, the spectral radiance can be expressed by[22]

$$I(o,\mu) = \epsilon_G B(T_G)\, e^{-\frac{\tau_1}{\mu}} + \frac{1}{\mu}\int_o^{\tau_1} B[\tau(T)]\, e^{-\frac{\tau}{\mu}}\, d\tau. \qquad (1)$$

B is the Planck function and $\cos^{-1}\mu$ the emission angle. All quantities in Eq. 1, except μ and T, depend on the wavenumber, ν. The optical depth τ is defined by

$$\tau(\nu,z) = \int_z^{\infty} \sum_i [k_i(\nu,z',T)\ \rho_i(z',T)]\, dz', \qquad (2)$$

where k_i and ρ_i are the absorption coefficient and density of gas i, and z and z' are altitudes. Eqs. 1 and 2 are valid only for monochromatic radiation; a convolution with the instrument function is required before computed and observed radiances can be compared.

The first term in Eq. 1 represents emission from a solid surface and the second term emission from atmospheric layers. The Galilean satellites, except Io, and the satellites of Saturn, except Titan, have virtually no atmosphere; therefore only the first term in Eq. 1 needs to be considered. The measured infrared spectra from these airless bodies follow reasonably closely the energy distribution of a blackbody; this allows a precise temperature measurement but says little about the chemical composition of the surface. Even Europa, which from ground-based near-infrared measurements[23] is known to have water ice on its surface, did not show the signatures of ice in the far infrared.[24] In contrast to this, small crystals of water ice suspended in the atmosphere of Mars showed strong characteristic signatures of ice,[25] as shown in Fig. 4. A similar phenomenon was observed with the fine dust suspended in the atmosphere of Mars.[9] The dust displayed prominent spectral features shortly after arrival of Mariner 9 during the great dust storm of 1971, but the features diminished with clearing and settling of the dust. While suspended, dust absorption and emission affected the spectrum by contrast against the warmer or cooler background, but while on the surface the temperature contrast was small and the spectral features had almost disappeared.

The only case where we have observed a surface emissivity effect with certainty is in the desert areas on Earth.[2,3] Even in the presence of an atmosphere, the surface may be observed in spectral regions where τ_1 is small compared to unity, as shown in Fig. 5. The variation of the surface emissivity with wavenumber gives a clue to the chemical composition. SiO_2 in coarse quartz sand shows strong reststrahlen features in the spectrum of the Sahara. Global maps of this feature, for example, illustrate the distribution of deserts on Earth.[26]

The thermal emission from Io is also predominantly from the surface. Only near 1350 cm^{-1} have SO_2 gas and possibly SO_2 ice crystals been detected by IRIS in a region containing a volcanic plume,[11] as shown in Fig. 6. Many Io spectra show surface emission from hot spots of higher than ambient temperatures indicating volcanic activity on a large scale.[10,24] Some of the low wavenumber features of Io have escaped identification so far.

We believe the solid (or liquid) surface of Titan is observed at approximately 550 cm^{-1}, with only a small atmospheric opacity due to the wings of pressure-induced nitrogen and hydrogen lines and residual absorption by methane clouds.[13,27]

Now we shall turn our attention to atmospheric emission, that is to the second term of Eq. 1, which dominates in spectral regions where τ_1 is large. The task of deriving atmospheric temperatures from a measurement of I_ν requires an inversion of the integral equation 1 which, in the early days of remote sensing, was often compared to the task of reconstructing an egg from its scrambled state. However, much has been learned about this process in the last decade[28] so that today the inversion technique is generally not a limiting factor in the interpretation of planetary spectra.

One can always compute a synthesized spectrum by assuming a vertical profile of temperature and a reasonable distribution of atmospheric constituents, comparing the calculated to the observed spectrum, making adjustments to the assumptions, and iterating the process until agreement exists across the spectrum. A careful error analysis must be performed because solutions are not always unique. All inversion procedures assume that the absorption coefficients of all absorbers involved are adequately known as functions of temperature and pressure. Line by line computational methods and molecular parameters are now available[29] for many molecules in the form of listings of line positions and strength on magnetic tape.[30] However, for many other molecules such listings are often incomplete or nonexistent. Some of the more complex hydrocarbons, which we found on Titan fall into the latter category; it makes interpretation of spectra and determination of abundances often difficult.[31,32] Even for CO_2, which has been studied extensively because of its importance for the retrieval of vertical temperature profiles in the Earth's atmosphere, it was necessary to include many very weak bands and even bands of isotopes, including ^{13}C and ^{17}O into our molecular models before the spectrum of the 667 cm^{-1} Martian CO_2 band, shown in Fig. 7, was fully understood.[33]

Extraction of the temperature profile from a planetary emission spectrum requires analysis of a spectral region where a single uniformly mixed gas of known abundance is the dominant emitter. In the terrestrial spectrum the high wavenumber side of the 667 cm^{-1} CO_2 band (see Figs. 1 and 5) is well suited for that purpose and has been the main spectral interval for temperature sounding on an operational basis. Weak absorption by O_3 and H_2O lines, also present in this region, can be accounted for in the analysis. As mentioned before, the same CO_2 band served our Mars investigation.[8] On Jupiter and Saturn pressure-induced absorption lines of hydrogen, the major constituent in those atmospheres, permitted retrieval of temperatures between 100 and 700 mb. The strong CH_4 band at 1304 cm^{-1} allowed extension of the profiles up to altitudes corresponding to a pressure of about 1 mb.[10,12,13]

On Titan matters are more complicated. Direct temperature retrieval in the CH_4 band is possible from the IRIS spectra between about 1 and 20 mb. For higher pressures no suitable spectral region was found for a direct temperature inversion. Pressure-induced hydrogen lines are present, but are very weak, and exist in a spectral region where other absorbers, probably methane clouds, interfere.[27] Fortunately, the Radio Science team on Voyager[34] obtained a T/m profile of Titan's atmosphere (T is the temperature and m the mean molecular weight). Combining this profile with IRIS derived temperatures yielded the actual temperature profile from 1 to 1600 mb, that is from the high stratosphere to the surface, as well as a mean molecular weight of about 28.6 AMU. The latter value suggests an N_2 atmosphere with an admixture of a heavier gas, possibly argon.[27] Vapor pressure considerations limit the stratospheric CH_4 content to $\sim$2.7%; in the troposphere the CH_4 content seems to be higher, but only about 0.6 of the saturation level.[27] This picture is consistent with a stratified cloud layer composed of CH_4 ice crystals just below the tropopause and a relatively clear zone below the cloud deck filled only with a slowly settling smog consisting mostly of solid hydrocarbons. Temperature profiles of Titan and other planets are summarized in Fig. 8.

After having established the temperature profile, that is after having solved Eq. 1 for $T(\tau)$ for a uniformly mixed known constituent, one may reverse the process and solve for the opacity distribuiton, $\tau(T)$, of an unknown

atmospheric constituent by using a spectral region where emission from the latter dominates. This has been done for water vapor and ozone on Earth[1,2,18] and for NH_3 on Jupiter.[35] However, in many cases the weakness of spectral features of minor constituents has only allowed establishment of their existence or mean abundances. The atmospheric composition of Titan is listed in Table 1.[27,32] Gases are also identified in the Titan spectra shown in Fig. 9 and 10.

In addition to gases which have specific features in the measured spectra, helium can be identified in an indirect way. Helium atoms colliding with hydrogen molecules change the shape of the broad pressure induced lines of hydrogen.[36] Analysis of the line shape of the H_2 features in the 200-600 cm^{-1} range has permitted the derivation of the helium abundances on Jupiter and Saturn. The mass fraction of helium on Jupiter was found to be 0.19 ± 0.05 from the IRIS spectra alone and 0.21 ± 0.06 from a technique which combines IRIS and Radio Science results.[37] For Saturn the IRIS spectra yielded a lower helium abundance of only 0.11 with an error not yet precisely determined, but probably smaller than on Jupiter.[13] Theories of the interior structure of the giant planets have predicted this depletion.[38,39,40] According to these theories the atmosphere of Saturn should be differentiated by gravitational forces, causing depletion of helium in the outer layers and enrichment in the interior. The sinking of helium liberates gravitational energy which is converted to heat and contributes to the excess of primordial heat emitted by both giant planets. On Jupiter, this excess of thermal radiation has been determined from IRIS data to be 1.67 ± 0.09 times the energy Jupiter receives from the Sun.[41] The IRIS analysis of the excess energy of Saturn has not yet been completed, but preliminary estimates and previous measurements by Pioneer[42] suggest that Saturn's excess energy fraction will be at least as large as Jupiter's.

The discussion of interesting results obtained by IRIS is far from complete. Time does not permit me to show the wind field derived from temperature data on Mars,[8,9] or the wind shear computations on Jupiter,[43] Saturn[43] and Titan,[44] or the dynamics of the Great Red Spot.[45] I will not discuss IRIS results on the rings of Saturn[13] or the topography of Mars.[8] In spite of these and other omissions, I hope I have given you an overview of

some of the highlights and shown to you the merits of Fourier transform spectroscopy in the thermal infrared.

I would like to mention that the IRIS data for the Voyager Jupiter encounter and the earlier missions are stored on magnetic tapes. Researchers may request copies from the Space Science Data Center at Goddard Space Flight Center, Greenbelt, MD 20771. Saturn data will become available to the scientific community in early 1982. I thank B. Conrath and J. Pearl for critically reading the manuscript.

Table 1. Atmospheric Composition of Titan
Inferred from Voyager IRIS[27,31,32]

Chemical Family	Gas	Wave Number (cm^{-1})	Approximate Mole Fraction
Major Constituents			
	Nitrogen, N_2	*	~ 0.85
	Argon, A	*	~ 0.12
	Hydrogen, H_2	350	2×10^{-3}
Carbon-Hydrogen			
	Methane, CH_4	1304	~3×10^{-2} **
	Ethane, C_2H_6	822	2×10^{-5}
	Propane, C_3H_8	748	1×10^{-5}
	Acetylene, C_2H_2	729	5×10^{-6}
	Ethylene, C_2H_4	950	8×10^{-7}
	Methyl Acetylene, C_3H_4	325,633	6×10^{-8}
	Diacetylene, C_4H_2	220,628	
Carbon-Hydrogen-Nitrogen			
	Hydrogen Cyanide, HCN	712	5×10^{-7}
	Cyanoacetylene, HC_3N	500,663	
Carbon-Nitrogen			
	Cyanogen, C_2N_2	233	

* Determined from mean molecular weight obtained in conjunction with Voyager Radio Science Investigation.[13,27,34]

** Variable with altitude, less than 2.7% in the stratosphere and possibly as high as 8% near the surface.

References

1. Hanel, R. and Conrath, B. "Interferometer Experiment on Nimbus 3: Preliminary Results", Science, Vol. 165, pp. 1258-1260, 1969.

2. Conrath, B. J., Hanel, R. A., Kunde, V. G. and Prabhakara, C., "The Infrared Interferometer Experiment on Nimbus 3", J. Geophys. Res., Vol. 75, No. 30, pp. 5831-5856, 1970.

3. Hanel, R. A., Conrath, B. J., Kunde, V. G., Prabhakara, C., Revah, I., Salomonson, V. V. and Wulford, G., "The Nimbus 4 Infrared Spectroscopy Experiment: 1. Calibrated Thermal Emission Spectra", J. Geophys. Res., Vol. 77, pp. 2639-2641, 1972.

4. Kunde, V. G., Conrath, B. J., Hanel, R. A., Maguire, W. C., Prabhakara, C. and Salomonson, V. V., "The Nimbus 4 Infrared Spectroscopy Experiment: 2. Comparison of Observed and Theoretical Radiances from 425-1450 cm^{-1}", J. Geophys. Res., Vol. 79, No. 6, pp. 777-784, 1974.

5. Prabhakara, C., Rodgers, E. B., Conrath, B. J., Hanel, R. A., Kunde, V. G., "The Nimbus 4 Infrared Spectroscopy Experiment: 3. Observations of the Lower Stratospheric Thermal Structure and Total Ozone", J. Geophys. Res., Vol. 81, No. 36, pp. 6391-6399, 1976.

6. Kempe, V., Oertel, D., Puder, J., Roseler, A., Sakatov, D. P. and Studemund, H., "Infrarot Fourier Spectrometer Sl-1 auf Meteor-25", Radio Fernsehen Electronik, Vol. 26, pp. 627-630, 1977.

7. Hanel, R. A., Conrath, B. J., Hovis, W. A., Kunde, V. G., Lowman, P. D., Pearl, J. C., Prabhakara, C., Schlachman, B., "Infrared Spectroscopy Experiment on the Mariner 9 Mission: Preliminary Results", Science, Vol. 175, pp. 305-308, 1972.

8. Hanel, R., Conrath, B., Hovis, W., Kunde, V., Lowman, P., Maguire, W., Pearl, J., Pirraglia, J., Prabhakara, C., Schlachman, B., Levin, G., Straat, P., and Burke, T., "Investigation of the Martian Environment by Infrared Spectroscopy on Mariner 9", Icarus, Vol. 17, pp. 423-442, 1972.

9. Conrath, B., Curran, R., Hanel, R., Kunde, V., Maguire, W., Pearl, J., Pirraglia, J., Welker, J., and Burke, T., "Atmospheric and Surface Properties of Mars Obtained by Infrared Spectroscopy on Mariner 9", J. Geophys. Res., Vol. 78, No. 20, pp. 4267-4278, 1973.

10. Hanel, R., Conrath, B., Flasar, M., Kunde, V., Lowman, P., Maguire, W., Pearl, J., Pirraglia, J., Samuelson, R., Gautier, D., Gierasch, P., Kumar, S., and Ponnamperuma, C., "Infrared Observations of the Jovian System from Voyager 1", Science, Vol. 204, pp. 972-976, 1979.

11. Pearl, J., Hanel, R., Kunde, V., Maguire, W., Fox, K., Gupta, S., Ponnamperuma, C., and Raulin, F., "Identification of Gaseous SO_2 and New Upper Limits for Other Gases on Io", Nature, Vol. 280, No. 5725, pp. 755-758, 1979.

12. Hanel, R., Conrath, B., Flasar, M., Herath, L., Kunde, V., Lowman, P., Maguire, W., Pearl, J., Pirraglia, J., Samuelson, R., "Infrared Observations of the Jovian System from Voyager 2", Science, Vol. 206, No. 4421, pp. 952-956, 1979.

13. Hanel, R., Conrath, B., Flasar, F. M., Kunde, V., Maguire, W., Pearl, J., Pirraglia, J., Samuelson, R., Herath, L., Allison, M., Cruikshank, D., Gautier, D., Gierasch, P., Horn, L., Koppany, R., Ponnamperuma, C., "Infrared Observations of the Saturnian System from Voyager 1", Science, Vol. 212, No. 4491, pp. 192-200, 1981.

14. Chaney, L. W., Drayson, S. R., and Young, C., "Fourier Transform Spectrometer-Radiative Measurement and Temperature Inversion", Appl. Opt., Vol. 6, pp. 347-349, 1967.

15. Hanel, R. A., and Chaney, L. W., "The Merits and Shortcomings of a Michelson Type Interferometer to Obtain the Vertical Temperature and Humidity Profile", Proc. XVII International Astronautical Congr., Madrid, Vol. 2, 1966.

16. Hanel, R., Schlachman, B., Clark, F. D., Prokesh, C. H., Taylor, J. B., Wilson, W. M., and Chaney, L., "The Nimbus III Michelson Interferometer", Appl. Opt., Vol. 9, No. 8, pp. 1767-1774, 1970.

17. Wark, D. Q., and Hilleary, D. T., "Atmospheric Temperature: Successful Test of Remote Probing", Science, Vol. 165, pp. 1256-1258, 1969.

18. Hanel, R. A., and Conrath, B. J., "Thermal Emission Spectra of the Earth and Atmosphere Obtained from the Nimbus 4 Michelson Interferometer Experiment", Nature, Vol. 228, pp. 143-145, 1970.

19. Hanel, R. A., Schlachman, B., Rodgers, D., Vanous, D., "The Nimbus 4 Michelson Interferometer", Appl. Opt., Vol. 10, pp. 1376-1381, 1971.

20. Hanel, R. A., Schlachman, B., Breihan, E., Bywaters, R., Chapman, F., Rhodes, M., Rodgers, D., and Vanous, D., "Mariner 9 Michelson Interferometer", Appl. Opt., Vol. 11, pp. 2625-2634, 1972.

21. Hanel, R., Crosby, D., Herath, L., Vanous, D., Collins, D., Creswick, H., Harris, C., and Rhodes, M., "Infrared Spectrometer for Voyager", Appl. Opt., Vol. 19, No. 9, pp. 1391-1400, 1980.

22. Hanel, R., Conrath, B., Gautier, D., Gierasch, P., Kumar, S., Kunde, V., Lowman, P., Maguire, W., Pearl, J., Pirraglia, J., Ponnamperuma, C., and Samuelson, R., "The Voyager Infrared Spectroscopy and Radiometry Investigation", Space Science Reviews, Vol. 21, pp. 129-157, 1977.

23. Pilcher, C. B., Ridgway, S. T. and McCord, T. B., "Galilean Satellites: Identification of Water Frost", Science, Vol. 178, pp. 1087-1089, 1972.

24. Pearl, J., and Sinton, W., "Hot Spots of Io", in The Satellites of Jupiter, D. Morrison, Ed., U. of Arizona Press, Tucson, AZ, 1981.

25. Curran, R., Conrath, B., Hanel, R., Kunde, V., Pearl, J., "Mars: Mariner 9 Spectroscopic Evidence for H_2O Ice Clouds", Science, Vol. 182, 381-383, 1973.

26. Prabhakara, C., and Dalu, G., "Remote Sensing of the Surface Emissivity at 9 μm over the Globe", J. Geophys. Res., Vol. 81, pp. 3719-3724, 1976.

27. Samuelson, R. E., Hanel, R. A., Kunde, V. G., and Maguire, W. C., "The Mean Molecular Weight and Hydrogen Abundance of Titan's Atmosphere", submitted to Nature, 1981.

28. Deepak, A., ed. "Inversion Methods in Atmospheric Remote Sounding", Academic Press, 1977.

29. Kunde, V. G., and Maguire, W. C., "Direct Integration Transmittance Model", J. Quant. Spectrosc. Radiat. Transfer, Vol. 14, pp. 803-817, 1974.

30. Rothman, L. S., Appl. Opt., Vol. 17, 3517-3518, 1978.

31. Maguire, W. C., Hanel, R. A., Jennnings, D. E., Kunde, V. G., and Samuelson, R. E., "Propane and Methyl Acetylene in Titan's Atmosphere", submitted to Nature, 1981.

32. Kunde, V. G., Aikin, A. C., Hanel, R. A., Jennings, D. E., Maguire, W. C., and Samuelson, R. E., "Identification of C_4H_2, HC_3N and C_2N_2 in the Atmosphere of Titan", submitted to Nature, 1981.

33. Maguire, W. C., "Martian Isotopic Ratios and Upper Limits for Possible Minor Constituents as Derived from Mariner 9 Infrared Spectrometer Data", Icarus, Vol. 32, pp. 85-97, 1977.

34. Tyler, G. L., Eshleman, V. R., Anderson, J. D., Levy, G. S., Lindal, G. F., Wood, G. E., and Croft, T. A., "Radio Science Investigations of the Saturn System with Voyager 1: Preliminary Results", Science, Vol. 212, No. 4491, pp. 201-105, 1981.

35. Kunde, V., Hanel, R., Herath, L., Maguire, W., Gautier, D., Baluteau, J. P., Marten, A., Chedin, A., Husson, N., and Scott, N., "The Lower Atmospheric Composition of Jupiter's North Equatorial Belt from the Voyager Investigation", in preparation.

36. Birnbaum, G., "Far Infrared Absorption in H_2-H_2 and H_2-He Mixtures", J. Quant. Spectrosc. Radiat. Transfer, Vol. 19, pp. 51-62, 1978.

37. Gautier, D., Conrath, B., Flasar, M., Hanel, R., Kunde, V., Chedin, A., and Scott, N., "The Helium Abundance of Jupiter from Voyager", J. Geophys. Res., accepted for publication, 1981.

38. Salpeter, E. E., "On Convection and Gravitational Layering in Jupiter and in Stars of Low Mass", Astrophys. J., Vol. 181, pp. L89-92, 1973.

39. Stevenson, D. J., and Salpeter, E. E., "The Phase Diagram and Transport Porperties for Hydrogen-Helium Fluid Planets", Astrophys. J. Suppl., Vol. 35, pp. 221-237, 1977.

40. Pollack, J. B., Grossman, A. S., Moore, R., and Graboske, H. C., "A Calculation of Saturn's Gravitational Contraction History", Icarus, Vol. 30, pp. 111-128, 1977.

41. Hanel, R. A., Conrath, B. J., Herath, L. W., Kunde, V. G., and Pirraglia, J. A., "Albedo, Internal Heat, and Energy Balance of Jupiter: Preliminary Results of the Voyager Infrared Investigation", J. Geophys. Res., accepted for publication, 1981.

42. Ingersoll, A. P., Orton, G. S., Munch, G., Neugebauer, G., Chase, S. C., "Pioneer Saturn Infrared Radiometer: Preliminary Results", Science, Vol. 207, No. 25, pp. 439-443, 1980.

43. Pirraglia, J. A., Conrath, B. J., Allison, M. D., Gierasch, P. J., "Global Thermal Structure and Dynamics of Saturn and Jupiter from Voyager Infrared Measurements", submitted to Nature, 1981.

44. Flasar, F. M., Samuelson, R. E., and Conrath, B. J., "Global Temperature Distribution and Dynamics of Titan's Atmosphere", submitted to Nature, 1981.

45. Flasar, F. M., Conrath, B. J., Pirraglia, J. A., Clark, P. C., French, R. G., and Gierasch, P. J., "Thermal Structure and Dynamics of the Jovian Atmosphere, I. The Great Red Spot", J. Geophys. Res., accepted for publication, 1981.

Figure Captions

Fig. 1. Planetary emission spectra. The uppermost spectrum was recorded by Nimbus 4 in 1970 over the mid-Atlantic Ocean. The second spectrum is of mid-latitudes of Mars recorded in 1972 by Mariner 9. The spectra of Jupiter, Saturn and Titan have been taken by Voyager 1 in 1979 and 1980 respectively.

Fig. 2. Conceptional diagram of IRIS. For Nimbus and Mariner the image motion conpensation and calibration mirror can be oriented so that IRIS sees the planet, deep space or an onboard blackbody.[15,19,20]

Fig. 3. Optical layout of the Voyager infrared instrument.[21] Calibration of the interferometer is accomplished by occasionally observing deep space and by precise temperature control of interferometer and telescope. Calibration of the radiometer is accomplished by occasionally viewing a diffusor plate mounted on the spacecraft and illuminated by the Sun.

Fig. 4. Mariner 9 spectra of Tharsis Ridge and Arcadia. Simultaneously taken images show partial cloudiness over Tharsis Ridge and little cloudiness over Arcadia. Calculated ice cloud spectrum in lower panel is for comparison.[25]

Fig. 5. Thermal emission spectra of Mars and Earth. a. and b. Martian south polar spectra after and during the dust storm. c. Martian mid-latitude spectrum with strong features due to silicate dust. d. Reststrahlen spectrum of Quartz sand. e. Sahara spectrum showing the reststrahlen feature in the atmospheric window between 1050 and 1250 cm^{-1}.[8]

Fig. 6. SO_2 gas on Io. Comparison of measured spectrum of Io with synthesized spectra in the vicinity of the ν_3 band of SO_2.[11]

Fig. 7. Comparison of measured and synthesized spectra of Mars in the region of the strong 667 cm^{-1} CO_2 band. The main spectral features are labeled with a three-digit number representing the isotope; thus $^{16}O^{13}C^{18}O$ is abbreviated 638. Unlabeled features are due to the main isotope $^{16}O^{12}C^{16}O$. The synthetic spectrum is displaced 20.3 K.[34]

Fig. 8. Atmospheric temperature profiles of Earth, Mars, Jupiter, Saturn, and Titan derived from infrared spectra and in the case of Titan in combination with Radio Occultation data. The profiles of Earth and Mars are typical of low latitudes; polar profiles are much colder and different in shape. Variations with latitude are generally smaller on the outer planets and on Titan.

Fig. 9. Average of 3 spectra of the Titan's north limb and two laboratory spectra of cyanoacetylene (HC_3N) and cyanogen (C_2N_2).[33] Other spectral features are labeled.

Fig. 10. Disk and north polar spectra of Titan and laboratory spectrum of diacetylene (C_4H_2).[33]

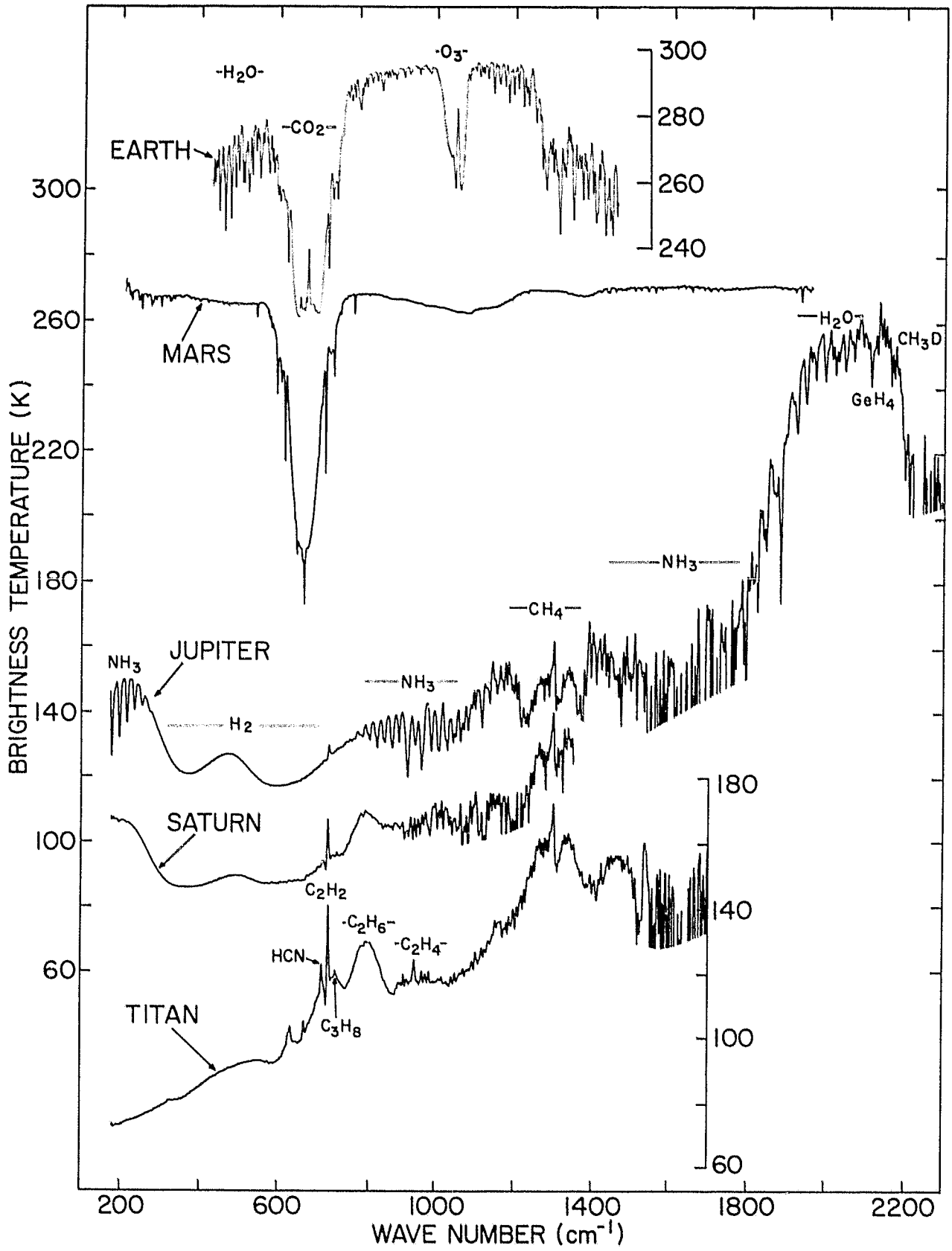
EARTH
-H2O-
-CO2-
-O3-
300
280
260
240
MARS
—H2O—
CH3D
GeH4
—NH3—
—CH4—
JUPITER
NH3
H2
SATURN
C2H2
-C2H6-
-C2H4-
HCN
C3H8
TITAN
BRIGHTNESS TEMPERATURE (K)
300
260
220
180
140
100
60
180
140
100
60
200
600
1000
1400
1800
2200
WAVE NUMBER (cm-1)

FIG. 1

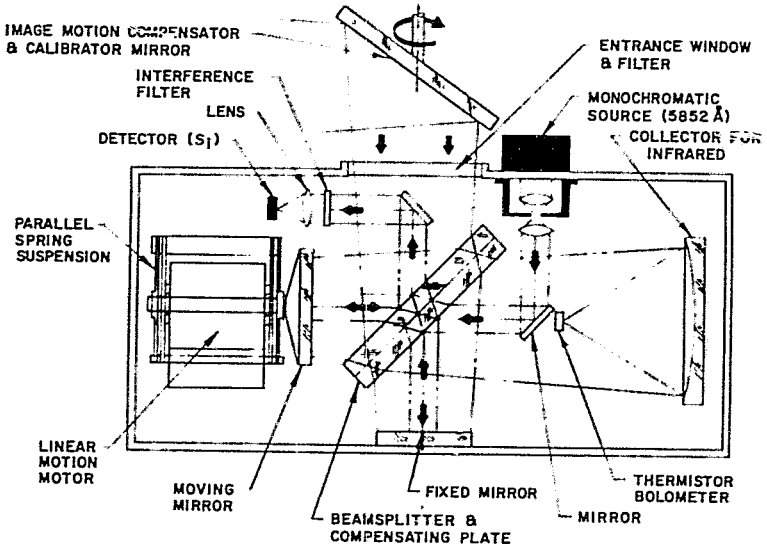
IMAGE MOTION COMPENSATOR & CALIBRATOR MIRROR
INTERFERENCE FILTER
LENS
DETECTOR (S_1)
ENTRANCE WINDOW & FILTER
MONOCHROMATIC SOURCE (5852 Å)
COLLECTOR FOR INFRARED
PARALLEL SPRING SUSPENSION
LINEAR MOTION MOTOR
MOVING MIRROR
BEAMSPLITTER & COMPENSATING PLATE
FIXED MIRROR
MIRROR
THERMISTOR BOLOMETER

FIG. 2

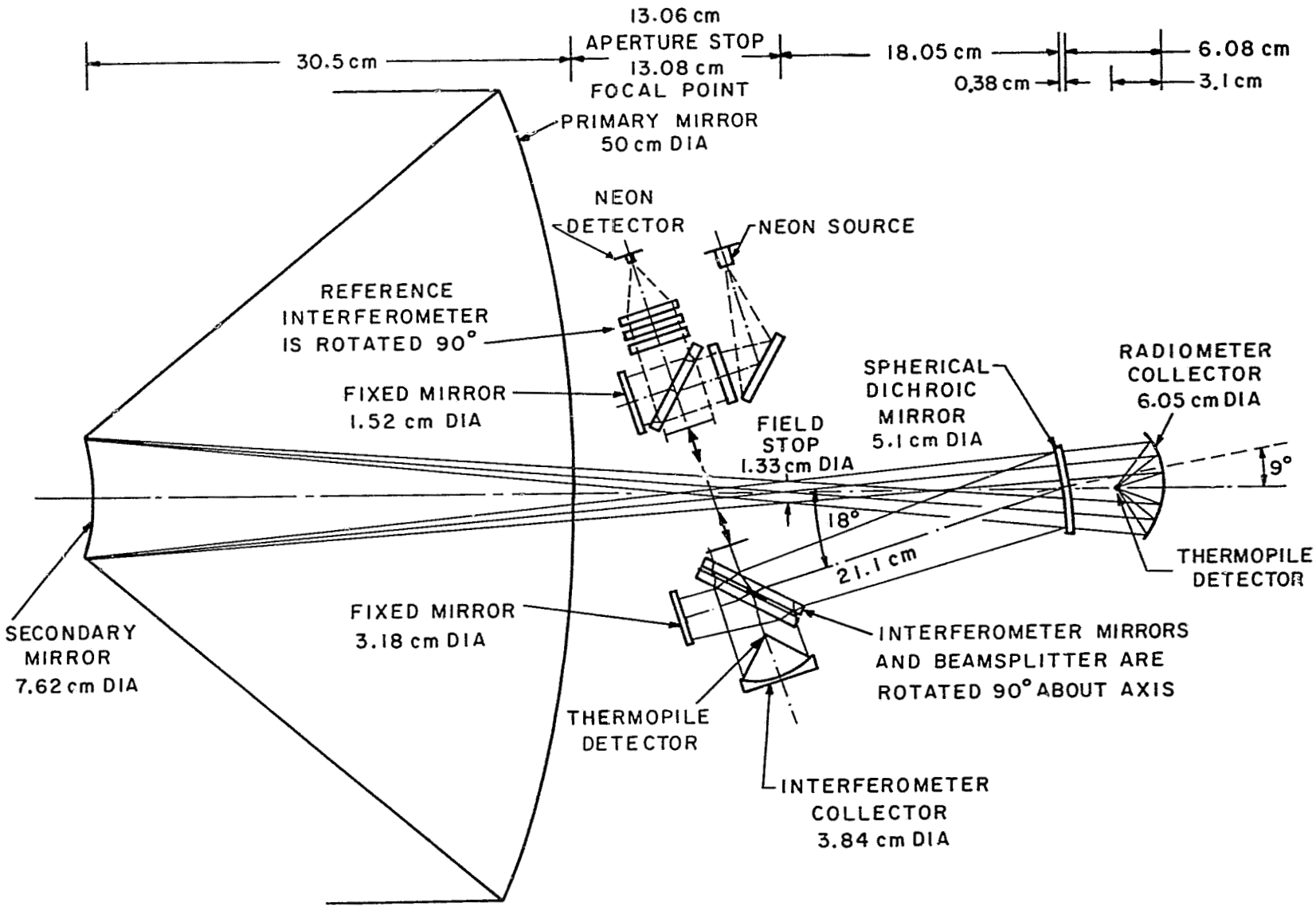
13.06 cm
APERTURE STOP
13.08 cm
FOCAL POINT
30.5 cm
18.05 cm
0.38 cm
6.08 cm
3.1 cm
PRIMARY MIRROR
50 cm DIA
NEON
DETECTOR
NEON SOURCE
REFERENCE
INTERFEROMETER
IS ROTATED 90°
FIXED MIRROR
1.52 cm DIA
FIELD
STOP
1.33 cm DIA
SPHERICAL
DICHROIC
MIRROR
5.1 cm DIA
RADIOMETER
COLLECTOR
6.05 cm DIA
9°
18°
21.1 cm
THERMOPILE
DETECTOR
SECONDARY
MIRROR
7.62 cm DIA
FIXED MIRROR
3.18 cm DIA
INTERFEROMETER MIRRORS
AND BEAMSPLITTER ARE
ROTATED 90° ABOUT AXIS
THERMOPILE
DETECTOR
INTERFEROMETER
COLLECTOR
3.84 cm DIA

FIG. 3

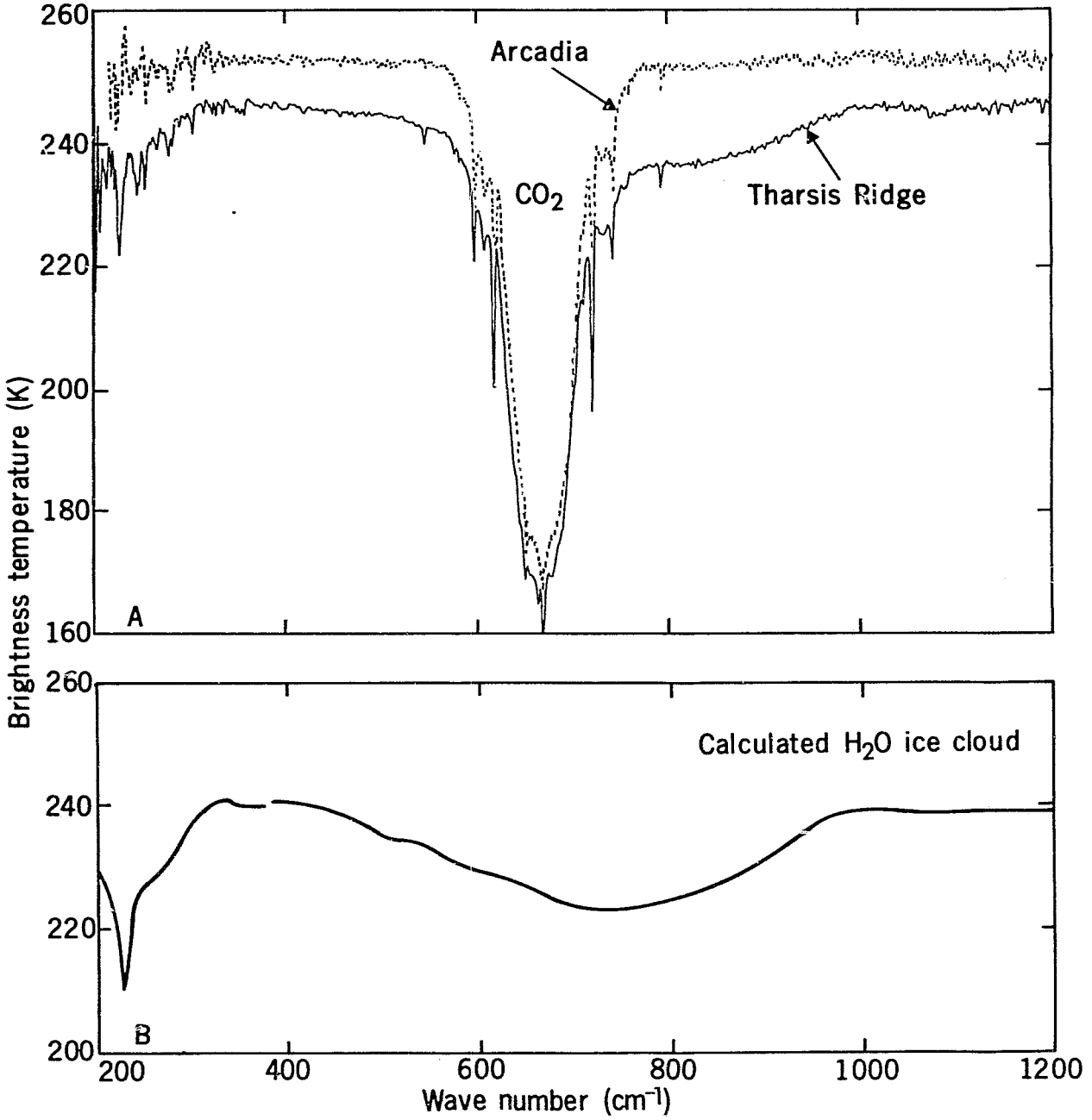
Arcadia
CO_2
Tharsis Ridge
A
Calculated H_2O ice cloud
B
Brightness temperature (K)
Wave number (cm^{-1})
260
240
220
200
180
160
200
400
600
800
1000
1200

Fig. 4

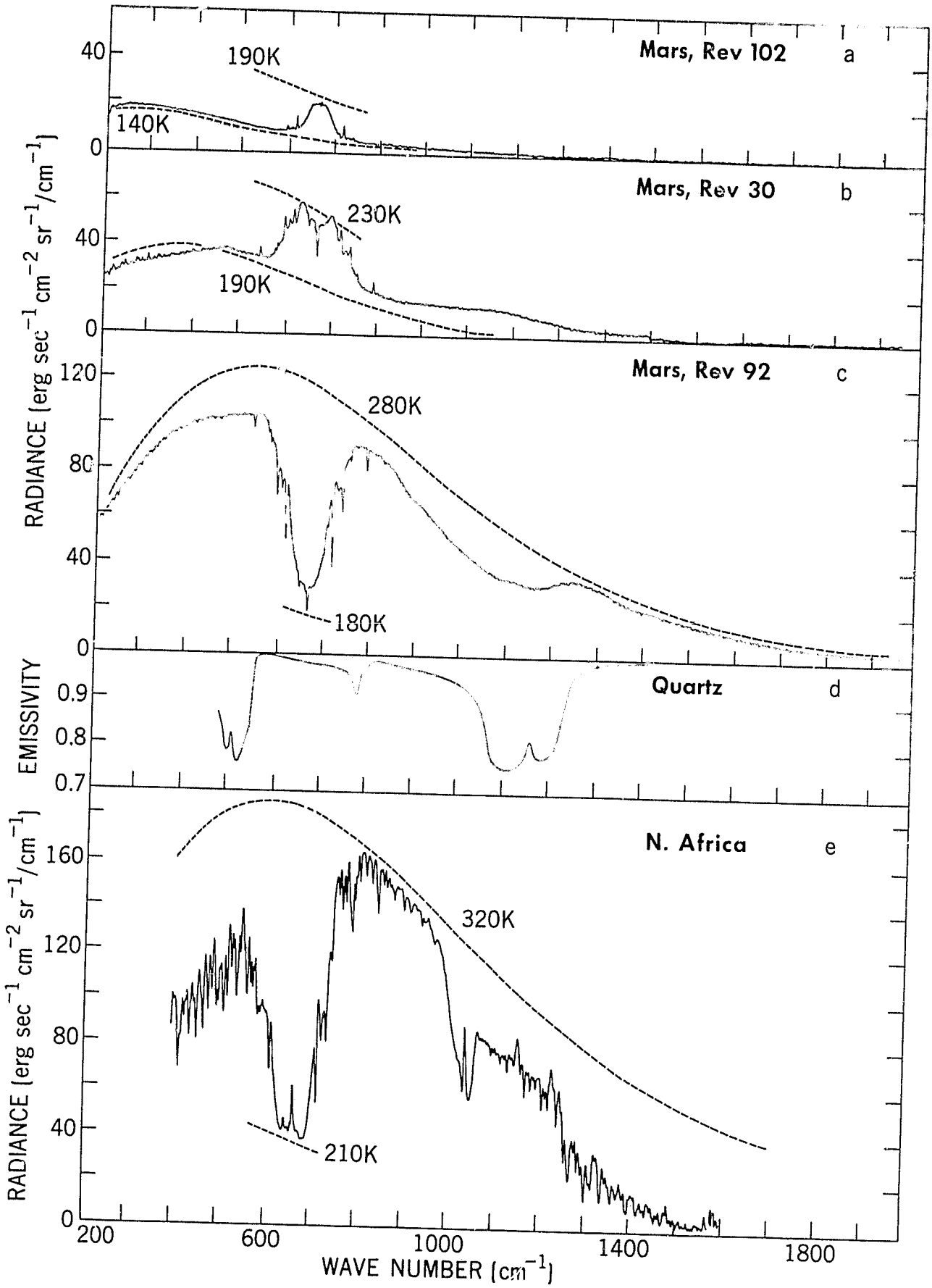
Mars, Rev 102
a
190K
140K
Mars, Rev 30
b
230K
190K
Mars, Rev 92
c
280K
180K
RADIANCE (erg sec^{-1} cm^{-2} sr^{-1}/cm^{-1})
EMISSIVITY
Quartz
d
N. Africa
e
320K
210K
WAVE NUMBER (cm^{-1})

FIG. 5

Fig. 6

RADIANCE (W cm^{-2} sr^{-1}/cm^{-1}) x 10^{8}
35
30
25
20
15
OBSERVED
SYNTHETIC
SO_2
U=0.1 CM-ATM
U=1.0 CM-ATM
1250
1350
1450
WAVE NUMBER (cm^{-1})

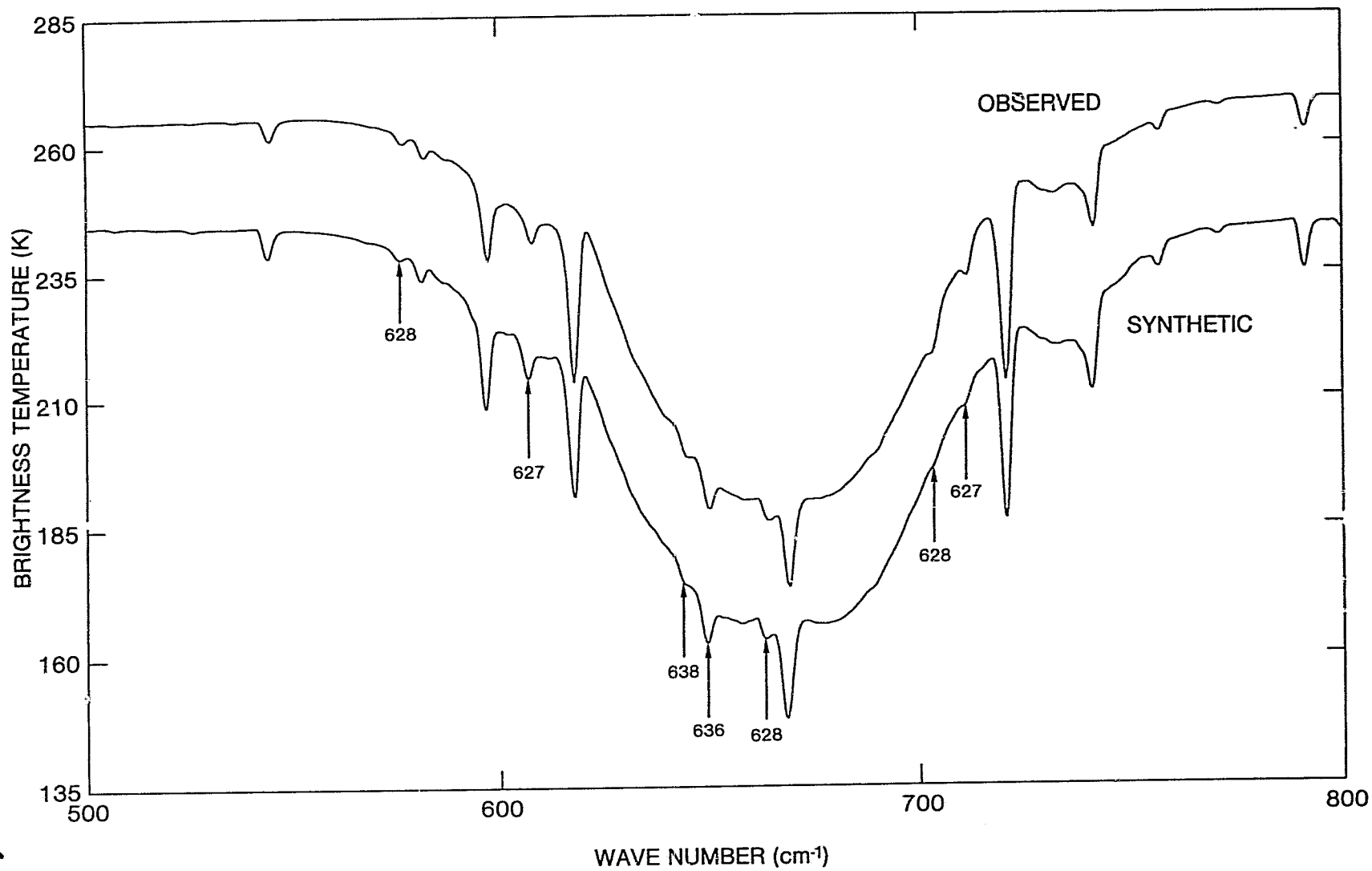
285
260
235
210
185
160
135
BRIGHTNESS TEMPERATURE (K)
500
600
700
800
WAVE NUMBER (cm-1)
OBSERVED
SYNTHETIC
628
627
638
636
628
628
627

Fig. 7

Fig. 8

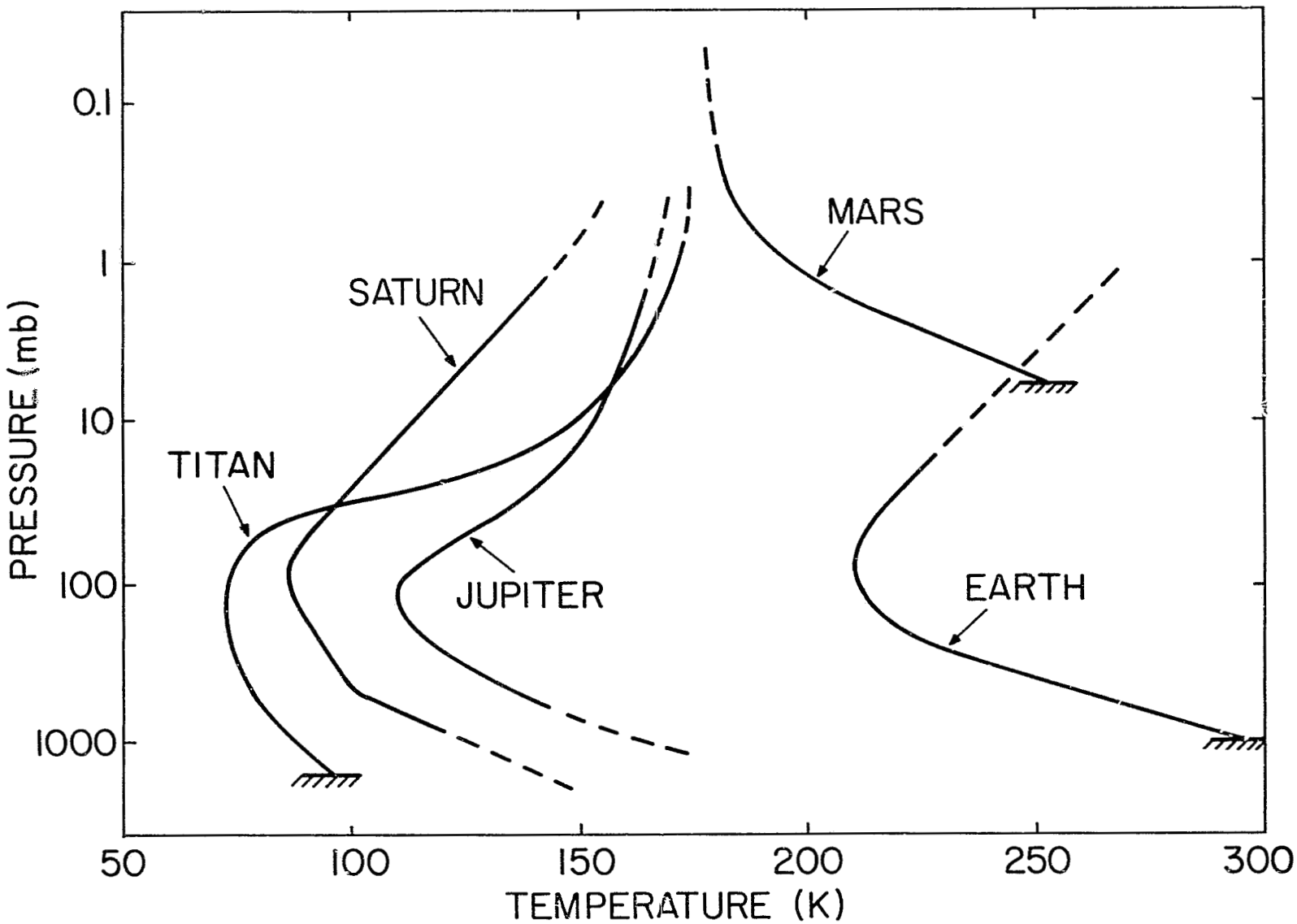
PRESSURE (mb)
0.1
1
10
100
1000
50
100
150
200
250
300
TEMPERATURE (K)
SATURN
MARS
TITAN
JUPITER
EARTH

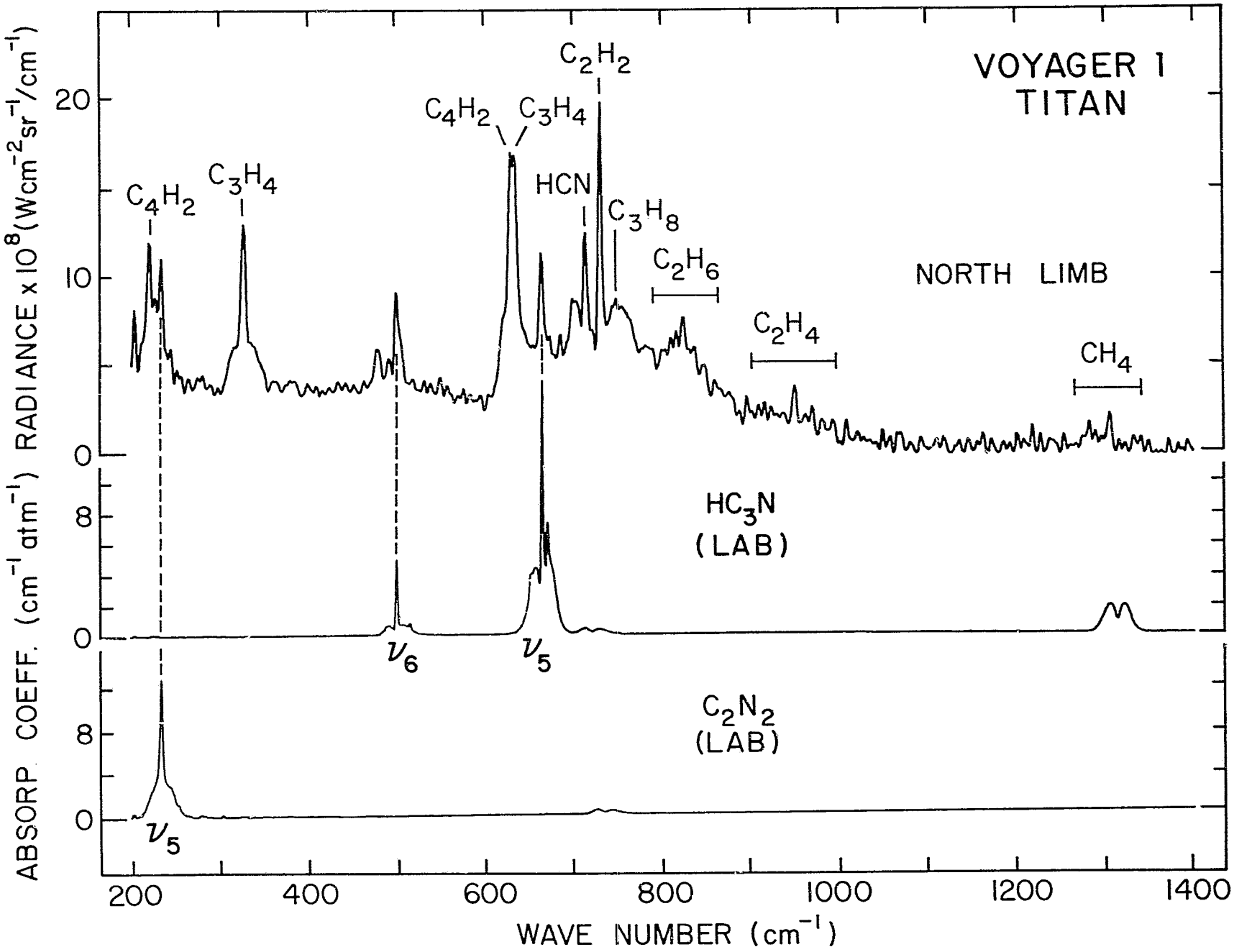
VOYAGER 1
TITAN
NORTH LIMB
C_4H_2
C_3H_4
C_4H_2
C_3H_4
C_2H_2
HCN
C_3H_8
C_2H_6
C_2H_4
CH_4
HC_3N
(LAB)
C_2N_2
(LAB)
ν_6
ν_5
ν_5
ABSORP. COEFF. (cm^{-1} atm^{-1}) RADIANCE x 10^8($Wcm^{-2}sr^{-1}/cm^{-1}$)
WAVE NUMBER (cm^{-1})
0
10
20
8
8
0
200
400
600
800
1000
1200
1400

FIG. 4

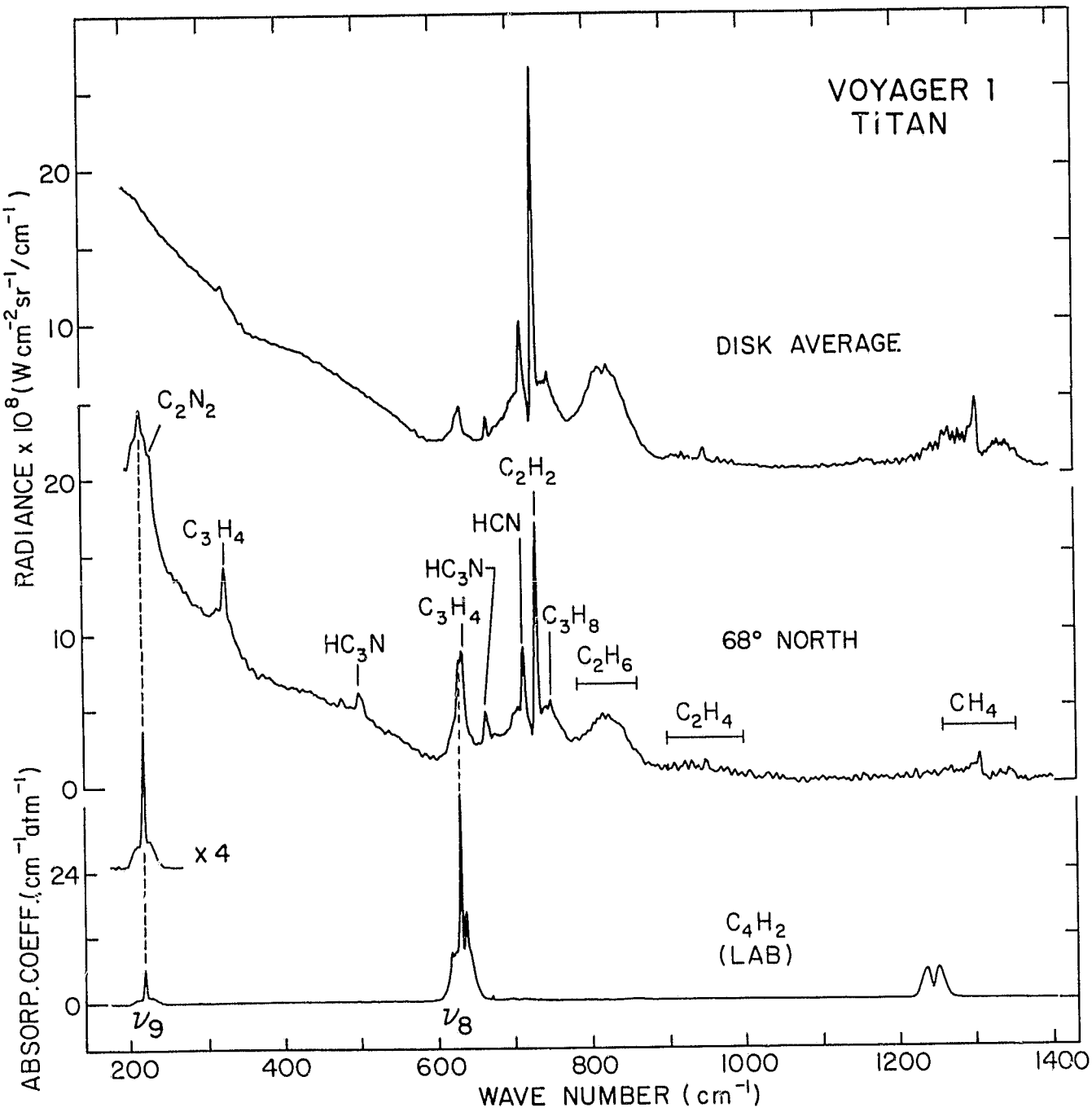
VOYAGER 1
TITAN
DISK AVERAGE
68° NORTH
C_4H_2
(LAB)
C_2N_2
C_3H_4
HC_3N
C_3H_4
HC_3N
HCN
C_2H_2
C_3H_8
C_2H_6
C_2H_4
CH_4
x 4
ν_9
ν_8
RADIANCE x 10^8 ($W\,cm^{-2}\,sr^{-1}/cm^{-1}$)
ABSORP.COEFF.($cm^{-1}atm^{-1}$)
WAVE NUMBER (cm^{-1})
200
400
600
800
1000
1200
1400

FIG. 10